Please cite this article in press as: Thomae et al., A Pair of Centromeric Proteins Mediates Reproductive Isolation in *Drosophila* Species, Developmental Cell (2013), http://dx.doi.org/10.1016/j.devcel.2013.10.001

Developmental Cell
Article

A Pair of Centromeric Proteins Mediates Reproductive Isolation in *Drosophila* Species

Andreas W. Thomae,[1] Georg O.M. Schade,[2,3,5] Jan Padeken,[2,3,5] Marc Borath,[1] Irene Vetter,[1] Elisabeth Kremmer,[4] Patrick Heun,[2] and Axel Imhof[1,*]
[1]Munich Centre of Integrated Protein Science and Adolf-Butenandt Institute, Ludwig Maximilians University of Munich, 80336 Munich, Germany
[2]Max-Planck Institute of Immunobiology and Epigenetics, 79108 Freiburg, Germany
[3]Faculty of Biology, Albert Ludwigs Universität Freiburg, 79104 Freiburg, Germany
[4]Helmholtz Zentrum Munich, Institute of Molecular Immunology, German Research Center for Environmental Health (GmbH), 81377 Munich, Germany
[5]These authors contributed equally to this work
*Correspondence: imhof@lmu.de
http://dx.doi.org/10.1016/j.devcel.2013.10.001

SUMMARY

Speciation involves the reproductive isolation of natural populations due to the sterility or lethality of their hybrids. However, the molecular basis of hybrid lethality and the evolutionary driving forces that provoke it remain largely elusive. The *hybrid male rescue* (*Hmr*) and the *lethal hybrid rescue* (*Lhr*) genes serve as a model to study speciation in Drosophilids because their interaction causes lethality in male hybrid offspring. Here, we show that HMR and LHR form a centromeric complex necessary for proper chromosome segregation. We find that the *Hmr* expression level is substantially higher in *Drosophila melanogaster*, whereas *Lhr* expression levels are increased in *Drosophila simulans*. The resulting elevated amount of HMR/LHR complex in hybrids results in an extensive mislocalization of the complex, an interference with the regulation of transposable elements, and an impairment of cell proliferation. Our findings provide evidence for a major role of centromere divergence in the generation of biodiversity.

INTRODUCTION

Postzygotic reproductive isolation is a major route to the formation of species in nature. How phenotypes as maladaptive as sterility and lethality can evolve under natural selection is best explained by the Dobzhansky-Muller (DM) model (Dobzhansky, 1951). It involves at least two loci that diverged in different natural populations and cause hybrid incompatibilies (HIs) when combined in hybrid offspring. Over the last decade, several HI genes have been identified in different model organisms (Bayes and Malik, 2009; Brideau et al., 2006; Long et al., 2008; Mihola et al., 2009; Schartl, 2008; Tang and Presgraves, 2009) with the key finding that many of these genes show signs of recurrent positive selection (Bayes and Malik, 2009; Maheshwari and Barbash, 2012; Phadnis and Orr, 2009). Increasing evidence suggests that these adaptive changes are driven by intragenomic conflicts (Brown and O'Neill, 2010; Crespi and Nosil, 2013). Possible conflict scenarios involve selfish DNA elements like transposable elements (Khurana et al., 2011; Kidwell et al., 1977) or centromeres that favor their own transmission, often at the expense of the overall fitness of the host organism (Fishman and Saunders, 2008; Hedges and Belancio, 2011; Pardo-Manuel de Villena and Sapienza, 2001). Such conflicts are supposed to promote the coevolution of compensatory mechanisms or factors, which may cause incompatibilities in hybrids (Malik and Henikoff, 2001; 2009). Unraveling the cellular function of HI genes is therefore crucial for uncovering the selective forces that drive their evolution and will yield mechanistic insights into the origin of species.

One of the best-characterized model systems to study speciation is the genus *Drosophila*. Male offspring from crosses between *Drosophila melanogaster* (*D.mel*) females and *Drosophila simulans* (*D.sim*) males die as larvae displaying reduced brain size and lacking imaginal discs, whereas females are viable but sterile (Sturtevant, 1920). Genetic studies suggested that the *D.mel Hmr* gene and the *D.sim Lhr* gene form a DM gene pair (Brideau et al., 2006; Davis et al., 1996) that causes this hybrid incompatibility by a yet-unknown molecular mechanism (Hutter and Ashburner, 1987; Maheshwari and Barbash, 2012; Watanabe, 1979). We therefore analyzed the HMR and LHR proteins at a molecular level in pure species as well as in hybrid animals.

RESULTS

HMR and LHR Form a Centromeric Complex

In order to investigate the molecular function of HMR and LHR, we purified proteins interacting with tagged HMR_{mel} and LHR_{mel} from *D.mel* Schneider cells (Figure 1A). Strikingly, LHR copurified with tagged HMR and vice versa, indicating that the observed genetic link is due to a protein-protein interaction. Furthermore, LHR and HMR display largely overlapping interaction profiles. Approximately 30% of the LHR-associated factors were also identified in HMR purifications, and even ~60% of the HMR interactors were shared by LHR. This suggests that a substantial amount of LHR and HMR proteins are involved in the formation of a common complex (Figure 1B). In order to identify proteins residing in such a complex, we performed a

Please cite this article in press as: Thomae et al., A Pair of Centromeric Proteins Mediates Reproductive Isolation in *Drosophila* Species, Developmental Cell (2013), http://dx.doi.org/10.1016/j.devcel.2013.10.001

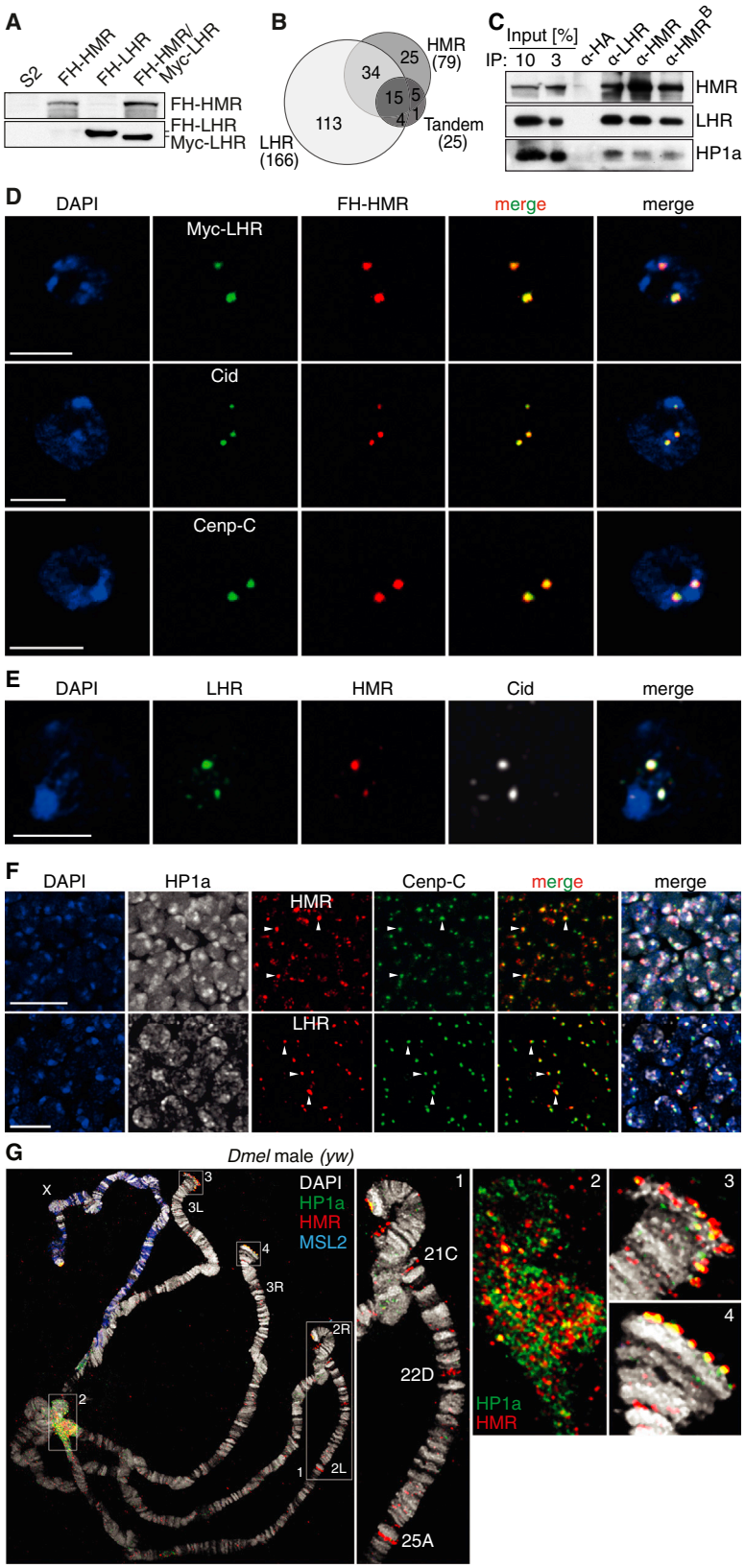

Figure 1. Characterization of a Centromeric HMR/LHR Complex

(A) Western blot showing the expression of FH-HMR, FH-LHR, and coexpression of FH-HMR/Myc-LHR in stable *D.mel* cell lines.

(B) Venn diagram of interaction partners.

(C) CoIP of endogenous HMR, LHR, and HP1a. CoIP reaction anti-HMR^{B} was treated with benzonase. Anti-HA IP served as a control.

(D) Colocalization of tagged HMR and LHR at the centromere. Single-section images of immunolocalizations using various antibodies.

(E and F) Colocalization of endogenous HMR/LHR and centromeric components in *D.mel* cells (E) and wing imaginal discs of *D.mel* (F). Closed arrows mark HMR colocalization with centromere foci.

(G) Immunolocalization of endogenous HMR, HP1a, and MSL2 on polytene chromosomes of *D.mel* males. Enlarged images of boxed regions (numbered from 1–4) are shown next to the overview image. White scale bars represent 5 μm.

See also Figure S1 and Tables 1 and S1.

Table 1. HMR/LHR Interaction Partners

Tandem	HMR/LHR
HP1a[a]	CG4887
Hmr	CG5792
Lhr	baf
Umbrea[a]	RpA-70
NLP	Su(var)3-7[a]
His4r	zip
glo	CG30007
His3.3B	cathD
CG4788	CG9775
Dcp1	CG3605
bel	mtSSB
CG5787	CG8578
ver	RpL27
CG7911	ytr
tral	Ku80
betaTub60D[b]	CG8878
Droj2[b]	BRWD3
Cenp-C[a,b]	CG9740
CG33213[b]	RpL21
lin-52[b]	Rala
His2B[c]	RPA2
Rm62[c]	RpS11
sqh[c]	pie
HP1b[d]	CG10916
Hlc[d]	su(Hw)
–	porin
–	Rab2
–	Rab7
–	AnxB10
–	RpL18A
–	CG16838
–	cher
–	moi
–	CG8108

Proteins listed in column "Tandem" were recovered in the tandem purification. Proteins listed in column "HMR/LHR" were copurified with HMR and LHR but were not recovered in the tandem purification. Proteins are sorted according to their enrichment in tandem and FLAG-HMR purifications, respectively. See also Table S1.

[a]Centromeric and pericentromeric proteins.

[b]Only recovered in FLAG-HMR and tandem purification.

[c]Only recovered in FLAG-LHR and tandem purification.

[d]Only recovered in tandem purification.

tandem-affinity purification from extracts of *D.mel* cells coexpressing differentially tagged HMR and LHR. This strategy led to the identification of 25 proteins residing in an HMR/LHR complex (Table 1 and Table S1 available online). Among those, we find several factors that bind to centromeric and pericentromeric regions like Cenp-C, HP1a, NLP, and Umbrea, pointing toward a centromeric function of the complex (Padeken et al., 2013; Ross et al., 2013; Vermaak and Malik, 2009).

Consistent with this hypothesis, we find both proteins colocalizing at centromeres when coexpressed as tagged transgenes (Figure 1D). Notably, if LHR is overexpressed without HMR, its distribution is different from the endogenous centromeric localization (compare Figures 1E and S1A), as seen by a lack of colocalization with the centromeric histone H3 variant Cid. This observation is in agreement with previous reports, describing LHR as a heterochromatin localized protein when expressed exogenously (Greil et al., 2007; Maheshwari and Barbash, 2012). HMR in contrast is capable of localizing to the centromere on its own (Figure S1B), showing that it is the main targeting component of the HMR/LHR complex in *D.mel*. To validate our findings for endogenous proteins, we generated highly specific antibodies against LHR and HMR (Figure S1C). Similar to the tagged factors, endogenous HMR and LHR form a stable complex with HP1, Umbrea, and Cenp-C (Figures 1C and S1D–S1E) and localize to the centromere (Figure 1E). The same centromeric localization is also observed in wing imaginal discs of third instar larvae (Figure 1F), a nonembryonal tissue with canonical mitotic cell cycles pointing to a role of the HMR/LHR complex for mitosis. On polytene chromosomes, HMR and LHR can also be detected at a few distinct euchromatic loci and at telomeres (Figures 1G and S1F), where they cannot be detected in mitotically cycling cells (Figure S1G).

The HMR/LHR Complex Has a Critical Function in Chromosome Segregation

Our finding that HMR and LHR form a complex at the centromere in mitotically cycling tissue prompted us to check whether those proteins play a role in chromosome segregation. We therefore depleted cells of either HMR or LHR using two different double-stranded RNAs (dsRNAs) leading to a substantial reduction of protein amounts (Figure S1C). Consistent with their function as a complex at centromeric chromatin, these knockdowns result in an increase of mitotic defects. The most frequently observed defect is lagging chromosomes with a minor occurrence of multipolar spindles or multinuclear cells, the distribution of which is similar to the control cells (Figures 2A–2C and S2A). In keeping with this, knockdown of *Hmr* in flies results in a 75%–80% drop in viability (Figure S2B). This is likely due to defects in cell proliferation, because a selective knockdown of *Hmr* in the posterior compartment of the wing disc frequently results in a complete loss of the posterior wing part (Figure S2C). A knockdown of *Lhr* in flies has only a subtle effect on viability. This was unexpected in light of the similar results obtained in cell lines, for both *Hmr* and *Lhr* RNAi (Figure S2B and see also Figures 2A–2C and 4B) and may be due to additional *Hmr* functions or simply reflect differences in RNAi efficiencies in the fly lines used.

The centromeric localization of the complex as well as its critical function for chromosome segregation may provide an explanation for the forces that drive its adaptive evolution (Maheshwari et al., 2008). Some essential centromere components also show such signs of positive selection (Malik and Henikoff, 2001; Dalal et al., 2007) underlining a strong evolutionary pressure to maintain a functional centromere in the context of highly variable centromeric DNA, which can differ substantially in sequence and size between species (Bergman et al., 2006; Sun et al., 1997, 2003).

Please cite this article in press as: Thomae et al., A Pair of Centromeric Proteins Mediates Reproductive Isolation in *Drosophila* Species, Developmental Cell (2013), http://dx.doi.org/10.1016/j.devcel.2013.10.001

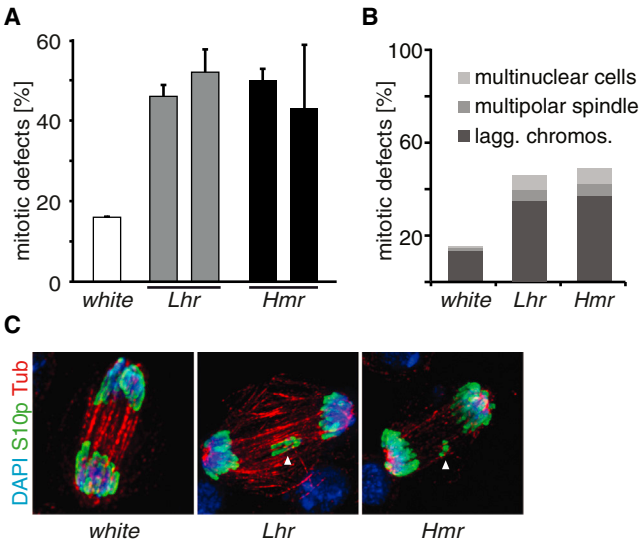

Figure 2. Knockdown of *Hmr* and *Lhr* Results in Increased Mitotic Defects

(A) Quantification of mitotic defects after knockdown of *Hmr* and *Lhr* in *D.mel* cells. Two nonoverlapping dsRNAs targeting *Lhr* or *Hmr* were used. dsRNA targeting the *white* gene served as control. Data are represented as mean ± SD.

(B) Types of mitotic defects observed after knockdown (see also Figure S2A).

(C) Images showing lagging chromosomes after *Hmr* and *Lhr* knockdown. A normal mitosis is illustrated in the leftmost image (*white* RNAi). White arrows indicate lagging chromosomes.

See also Figure S2.

Despite the strong divergence, centromeres are characterized by a conserved and unique epigenetic structure. Densely packed heterochromatin surrounds the inner centromere region, which is characterized by the presence of a special histone H3 variant termed Cenp-A (Cid). This architecture is crucial for centromere function and chromosome segregation (Olszak et al., 2011). As problems with proper chromosome segregation arise after *Hmr* and *Lhr* knockdown, we asked whether these defects are caused by an interference with centromere architecture. However, the localization of the inner centromere protein Incenp, the constitutive centromere protein Cenp-C as well as the outer kinetochore components Polo, Rod, and Ndc80 do not change upon *Hmr* and *Lhr* knockdown (Figure 3A). We furthermore investigated the possibility that the HMR/LHR complex might serve as a chaperone or a priming factor to facilitate the incorporation of newly synthesized Cid using a cell line expressing SNAP-tagged Cid (Mellone et al., 2011). Yet, neither *Hmr* nor *Lhr* knockdown interferes with the incorporation of newly synthesized Cid (Figures 3B–3D). In addition, the fact that HMR and LHR are not present on metaphase chromosomes argues against an immediate role of HMR/LHR during mitosis (Figures S3A and S3B). Live-cell imaging of cells expressing fluorescently tagged HMR, LHR, and Cid reveals that the HMR/LHR complex disappears upon mitotic entry and rebinds the centromere after completion of mitosis (Figure S3B; Movie S1). This led us to the conclusion that the HMR/LHR complex exerts its centromeric function during interphase.

The HMR/LHR Complex Acts as a Transcriptional Repressor of Transposable Elements

Experiments in fission yeast show that the transcription of centromeric regions during interphase is highly regulated and affects centromeric function (Chen et al., 2008; Scott et al., 2006; 2007). As the HMR/LHR complex also interacts with HP1a and other known repressor proteins (Figures 1B and 1D; Table 1), we wondered whether its role at centromeres is of a repressive nature. To analyze whether HMR and LHR can act as transcriptional repressors, we targeted the proteins to a luciferase reporter plasmid and measured their ability to repress transcription. Indeed, when either protein is recruited to the reporter, transcriptional activity is substantially decreased and declines further when the corresponding partner is coexpressed (Figure 4A). As transposable elements are strongly enriched at centromeres (Bergman et al., 2006), we investigated whether HMR and LHR repress these elements under physiological conditions. Indeed, a knockdown of *Hmr* or *Lhr* results in an increased expression of a subset of transposable elements (TEs) (Figure 4B). The increase is comparable to a knockdown of the RNAi component *Ago2*, which is known to function in the silencing of transposable elements (Czech et al., 2008). Although we do not know the molecular mechanism by which HMR and LHR repress transcription, their interaction partners, as well as their localization pattern, suggest that they are involved in setting up a repressive chromatin environment at the centromere. In this light, it is noteworthy that a similar derepression of transposable elements is also observed upon knockdown of the NLP subunit of the HMR/LHR complex, which has been shown to be important for centromere clustering (Padeken et al., 2013). However, because neither *Hmr* nor *Lhr* knockdown affects centromere clustering they are likely involved in a downstream process (data not shown).

Our experiments show that HMR and LHR form a stable complex at the centromere whose dosage is critical for proper mitotic divisions in *D.mel*. The centromeric function explains the selective forces that drive their adaptive evolution similar to other known centromeric factors. However, it does not resolve why these factors cause lethality in a hybrid genetic background.

The DM model proposes that hybrid incompatibilities arise as a result of the divergent evolution of speciation genes. We therefore aimed to uncover features that are different between HMR and LHR in both species. Coimmunoprecipitation experiments indicate that the interaction between HMR and LHR is conserved in *D.sim* (Figure 5A). Moreover, a comparison of the LHR_{mel} and LHR_{sim} interactome in *D.mel* cells revealed that the two orthologs interact with identical proteins including HMR_{mel} (Figures 5B and 5C; Table S1). Localization studies furthermore show that an interspecific HMR_{mel}/LHR_{sim} complex localizes to the centromere in *D.mel* cells similar to the intraspecific complex (Figure 5D). This strong functional conservation of LHR is consistent with previous findings showing that the overexpression of Lhr_{mel} can suppress the $Lhr^{1}{}_{sim}$-dependent hybrid male rescue (Brideau and Barbash, 2011). On the contrary, because sibling *Hmr* alleles do not kill hybrid males rescued by an Hmr_{mel} mutation, it was concluded that *Hmr* must have gained a species-specific function in *D.mel*. Surprisingly, immunolocalization analysis with tagged HMR/LHR orthologs did not reveal obvious species-specific differences (Figures 5D and 5E). When coexpressed,

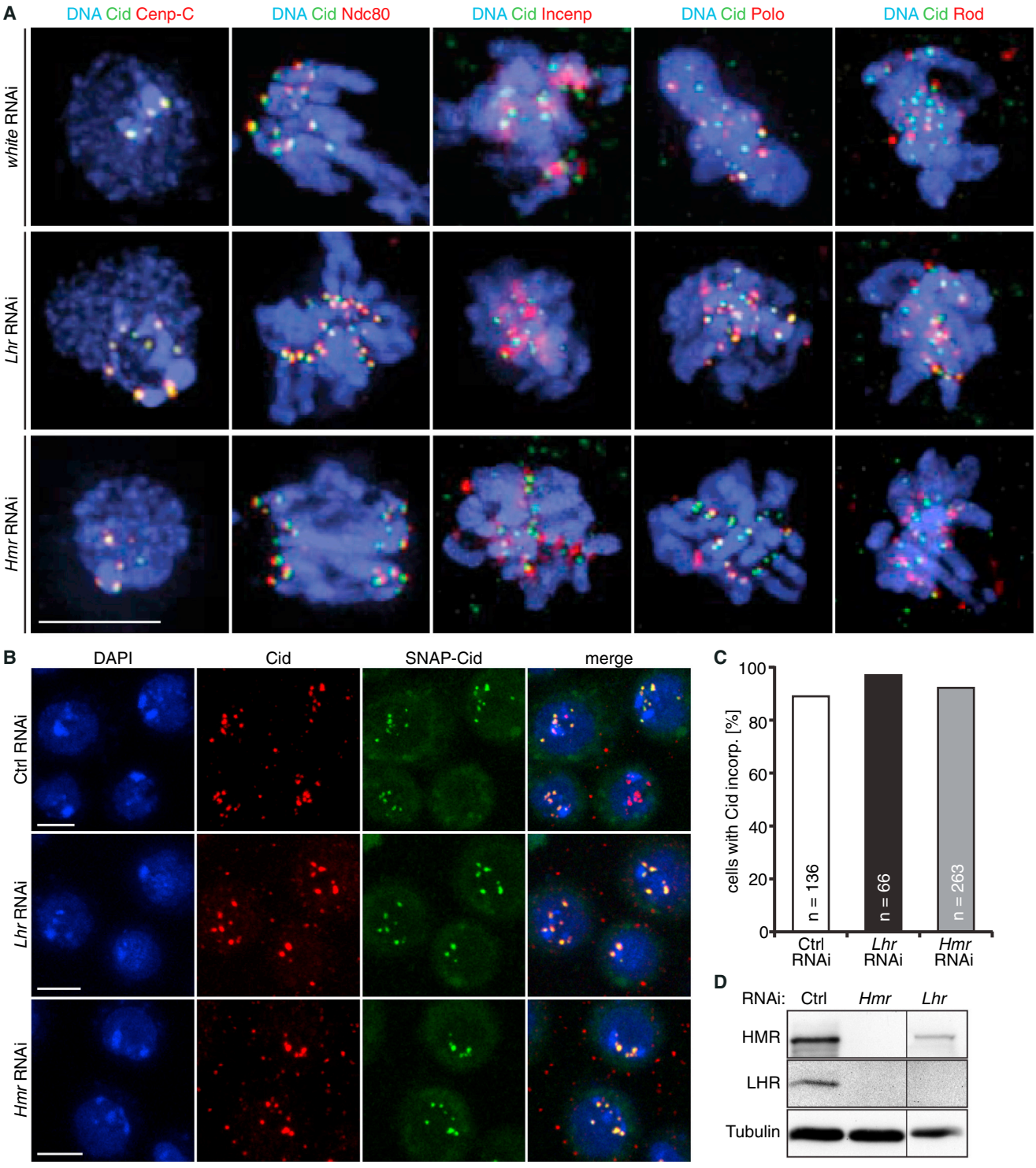

Figure 3. Unchanged Cid Incorporation and Localization of Known Centromere/Kinetochore Components after Knockdown of *Hmr* and *Lhr*

(A) Localization of known centromere/kinetochore components after *white*, *Hmr*, and *Lhr* knockdown.

(B) Incorporation of newly synthesized (SNAP-)Cid after Ctrl, *Hmr*, or *Lhr* RNAi.

(C) Quantification of cells displaying SNAP-Cid incorporation after RNAi. The number of cells investigated is given (n).

(D) Western blot demonstrating that RNAi reduces HMR/LHR levels. White scale bars in (A) and (B) represent 5 μm.

See also Figure S3.

Please cite this article in press as: Thomae et al., A Pair of Centromeric Proteins Mediates Reproductive Isolation in *Drosophila* Species, Developmental Cell (2013), http://dx.doi.org/10.1016/j.devcel.2013.10.001

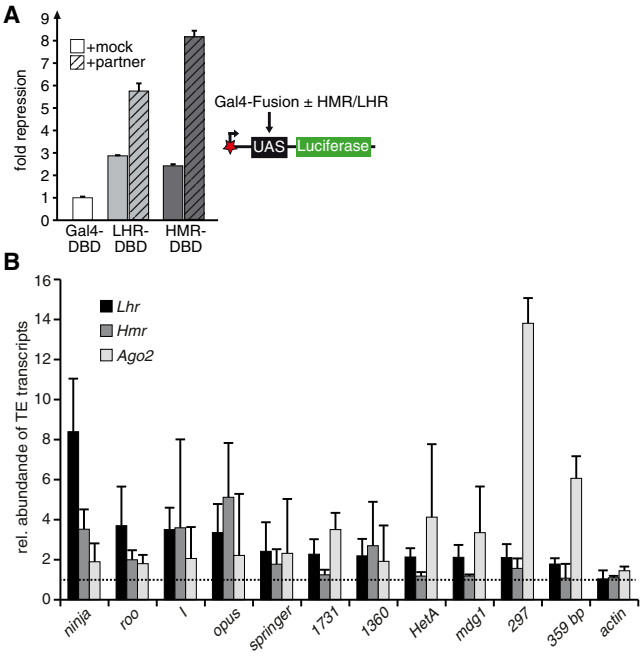

Figure 4. HMR and LHR Form a Repressor Complex that Silences Transposable Elements

(A) HMR and LHR cooperate in silencing of a Luciferase reporter. +partner (shaded bars) indicates cotransfection of FLAG-LHR with GAL4-HMR and vice versa. Data represent mean ± SD fold repression from three biological replicates.

(B) Abundance of transcripts from repetitive elements in S2 cells after *Hmr*, *Lhr*, and *Ago2* RNAi. Shown is the fold change after normalization to *white* RNAi and genomic copy number. Error bars indicate SD of three biological replicates.

HMR/LHR from *D.mel* and *D.sim* are capable of localizing to centromeres of their own as well as their sister species. This suggests that even though the factors are fast evolving many features are conserved. Such conservation is further supported by the findings that (1) Hmr_{sim} can partially complement the fertility defect of *D.mel Hmr* mutant females (Aruna et al., 2009), and (2) the *Hmr* allele Hmr^2 rescues lethal hybrid males due to two amino acid mutations with the critical residue (E371) that is located in HMR's third out of four MADF domains, being conserved between the orthologs (Aruna et al., 2009). Strikingly, we find that the Hmr^2 gene product almost completely lost its centromeric localization (Figures S4A and S4B). Hence, the same activity that confers HMR's centromere binding also leads to the incompatibility observed in hybrid males.

Because our LHR-specific immunofluorescence grade antibody does not recognize LHR_{sim} (Figure S4C), we were only able to investigate the localization of tagged LHR_{sim}. Similar to what we observe in *D.mel* cells (Figure S1A), tagged LHR_{sim} localizes to heterochromatin and not to centromeres, when *Hmr* is not coexpressed (Figure 5F).

HMR and LHR Have Inverted Species-Specific Expression Levels

We next investigated the localization of endogenous HMR_{sim} in *D.sim* cells by using a monoclonal HMR antibody that recognizes HMR_{sim} and HMR_{mel} with similar sensitivity (Figure S4D). In addition to a prominent staining of a noncentromeric region, we observe a centromeric localization of endogenous HMR in *D. sim* cells similar to the ectopic expression (Figures 5G and S4E, lower panel). However, we also noticed that the immunolocalization signal intensities were greatly reduced compared to those in *D.mel* cells. For a better comparison of the signal intensities, *D.mel* cells, marked by their expression of GFP-CID, were mixed with *D.sim* cells and simultaneously stained with the anti-HMR antibody (Figure S4E). A comparison of protein levels by immunoblotting confirmed that HMR levels are much higher in cell lines derived from *D.mel* compared to *D.sim* (Figure 6A). This raises the possibility that HMR's centromeric function is less important for *D.sim.* In good agreement with this hypothesis, the reduction of neither *Hmr* nor *Lhr* levels (although moderate) increases the frequency of mitotic defects in these cells (Figure S4F).

Consistent with the findings obtained in cell lines, the higher expression level of HMR in *D.mel* is also observed in extracts prepared from third instar larval brains (Figure 6B). In contrast, LHR levels are much higher in *D.sim* (Figure 6B), which is in line with the proposed asymmetric hybrid lethal effects of *Lhr* orthologs (Maheshwari and Barbash, 2012). Based on these results, we conclude that the divergent evolution led to an inverted species-specific *Hmr* and *Lhr* expression. These marked expression differences manifest themselves in increased amounts of the LHR/HMR complex in hybrid animals (Figures 6B and 6C). Because *Hmr* is a dosage-compensated gene on the X chromosome (Kharchenko et al., 2011), male hybrids containing a single *D.mel* X chromosome very likely express even higher levels of *Hmr* than females that contain one copy of Hmr_{mel} and one copy of Hmr_{sim}. This could explain the puzzling asymmetric lethality of male hybrids and would further predict that an additional Hmr_{mel} gene copy would kill female hybrids. Indeed, we observe complete lethality in female hybrids (Figure 6E) after introducing a single additional autosomal copy of the Hmr_{mel} gene expressed from its endogenous promoter. This result supports previous hypotheses, which were based on interspecific crosses using *D.mel* chromosomal duplication lines and claim, that increasing the Hmr_{mel} dosage has a negative effect on hybrid viability (Barbash et al., 2000; Hutter et al., 1990).

When we measured the levels of HMR and LHR in hybrids or *D.mel* larval brains that carry hypomorphic alleles of *Hmr*, we noticed that they also contain less LHR (Figure 6B, lanes 1, 5, and 6, and Figure 6C). The same effect is also seen when tissue culture cells are depleted of HMR or LHR using RNAi, suggesting that the levels of the two proteins are highly dependent on each other (Figure 6D). Surprisingly this effect is not observed in *D.sim* (Figure 6B, lane 3), where LHR is stable despite a much lower amount of HMR (see Discussion).

Overexpression of HMR and LHR Results in a Delocalization of the HMR/LHR Complex in Flies

We next investigated the molecular and cellular effects of the HMR/LHR complex under overexpression conditions. Surprisingly, the overexpression of HMR and LHR results in an increase in mitotic defects in tissue culture cells (Figures 7A and 7B) and a higher number of transcripts from transposable elements

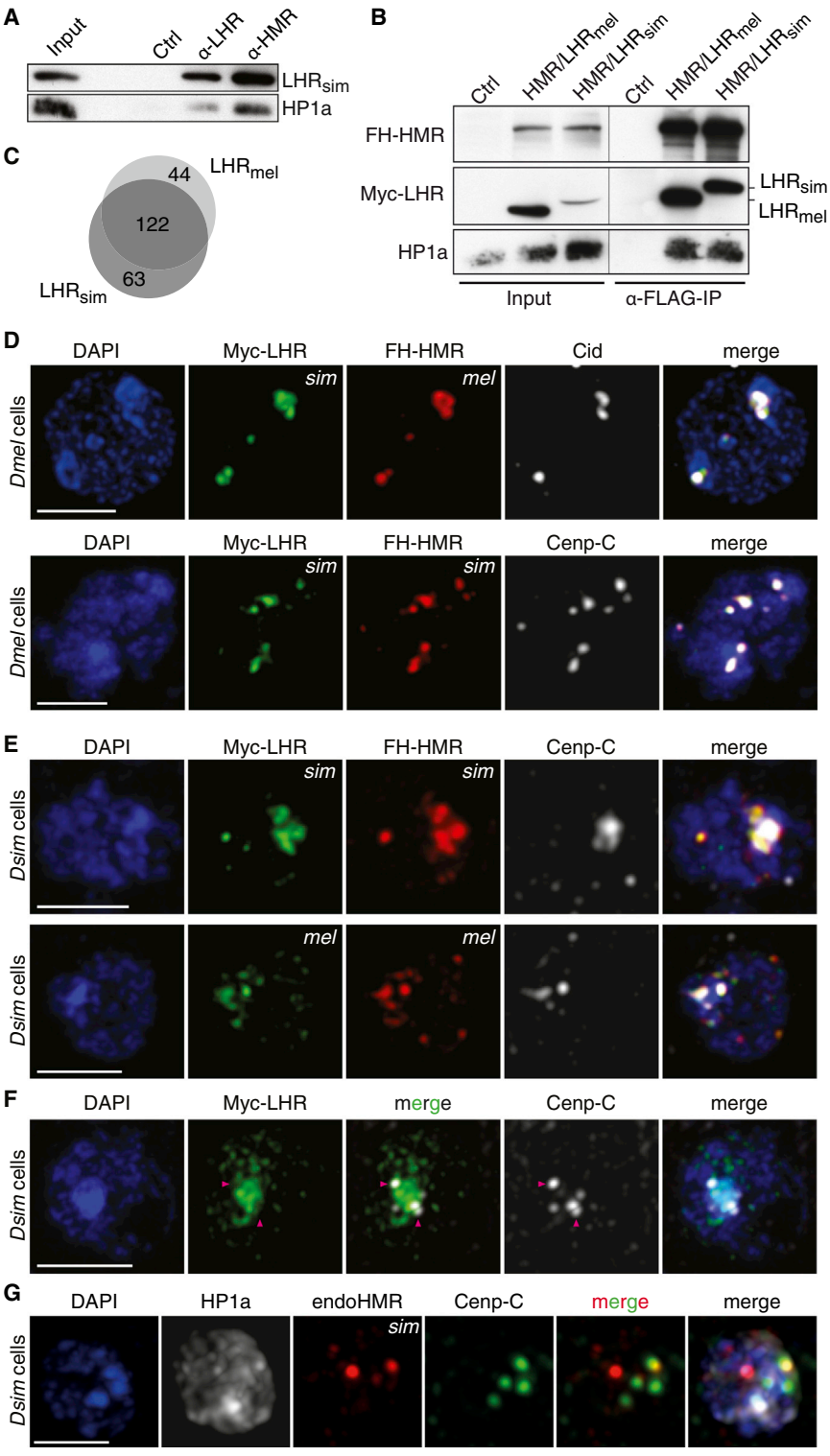

Figure 5. Conservation of Interactions and Localization of HMR and LHR Orthologs

(A) HMR_{sim} and LHR_{sim} coimmunoprecipitate in nuclear extracts from *D.sim* cells.

(B) Coimmunoprecipitation of Myc-tagged LHR orthologs with FH-HMR_{mel}.

(C) Comparison of LHR_{mel} and LHR_{sim} interactomes in *D.mel* nuclear extracts.

(D) Centromeric colocalization of Myc-LHR_{sim} with FH-HMR_{mel} and FH-HMR_{sim} in *D.mel* cells.

(E) Centromeric colocalization of HMR and LHR orthologs in *D.sim* cells.

(F) Heterochromatic localization of Myc-LHR_{sim} without HMR_{sim} coexpression in *D.sim* cells.

(G) Localization of endogenous HMR_{sim} in *D.sim* cells. White scale bars in (D) and (E) represent 5 and 3 μm, respectively.

See also Figure S4 and Table S1.

(Figure 7C) similar to the effects we observe when HMR and LHR levels are reduced (Figures 2A and 4B). As hybrids display increased levels of the HMR/LHR complex, we would expect to see similar effects at least in hybrid males. Mitotic defects in hybrids are difficult to assess, as hybrid males, in particular, are characterized by almost complete absence of imaginal discs and display reduced brain size with an extremely low frequency of cells in S phase and especially mitosis. These features are diagnostic for a defect in cell proliferation, and it has been suggested that hybrid cells are arrested in G1 or G2 phase (Baker, 1989; Bolkan et al., 2007).

Moreover, when we measured the RNA derived from transposable elements in hybrid males or females, we observed a massive increase in transposon transcripts, which is reduced in flies expressing lower levels of HMR (Figure 7D). Because these effects are not sex specific, we would conclude that the deregulation of transposable elements might affect the overall fitness of hybrids and potentially female fertility but is presumably not the main cause of hybrid male lethality.

Our finding that a mutation in *Hmr* that rescues hybrid male lethality also abrogates HMR's centromeric localization (Hmr^2 allele, see Figure S4A), suggests that the binding activity of HMRs third MADF domain might be problematic in hybrids. This prompted us to investigate HMR's binding behavior in hybrids. Thus, we stained polytene chromosomes isolated from either pure species or hybrid male third instar larvae using a monoclonal anti-HMR antibody. In contrast to pure species *D.mel*, where HMR binding is confined to the chromocenter, the telomeres, and very few distinct interbands (Figures 1G and 7E), HMR is bound to numerous interband regions along all chromosome arms in hybrids (Figures 7E and S5A). The virtually complete loss of signal in hybrid females from *D.mel*

Please cite this article in press as: Thomae et al., A Pair of Centromeric Proteins Mediates Reproductive Isolation in *Drosophila* Species, Developmental Cell (2013), http://dx.doi.org/10.1016/j.devcel.2013.10.001

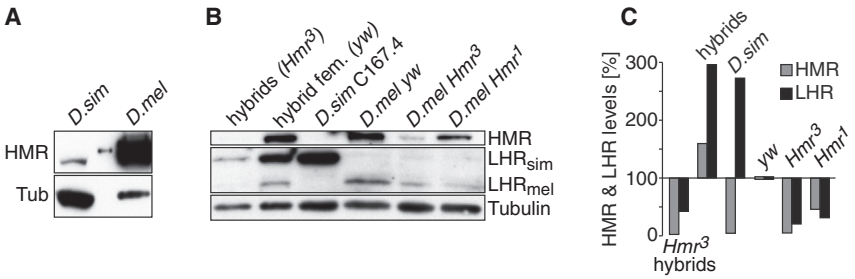

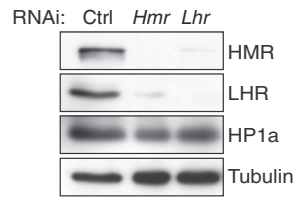

E

D.mel female parent	F1 hybrid offspring females		F1 hybrid offspring males	
#*yw*	431		0	
yw	216		0	
#*Hmr*^{3}	510		166	
Hmr^3	240		111	
	BAL	*Hmr*$^+$	BAL	*Hmr*$^+$
#*Hmr*^{3}; *Hmr*$^{+t9.5}$ /BAL	433	330	60	0
Hmr^3; *Hmr*$^{+t9.5}$ /BAL	60	61	46	0
yw; *Hmr*$^{+t9.5}$ /BAL	193	0	1*	0
yw; *Hmr*$^{+t9.5}$ /BAL	41	0	0	0

Figure 6. Increased HMR/LHR Dosage Due to Inverted Species-Specific *Hmr* and *Lhr* Expression Causes Hybrid Lethality

(A and B) Divergence of HMR and LHR levels in *D.mel* and *D.sim* cell lines (A) and larval brains (B).

(C) Quantification of HMR and LHR levels in hybrids and *D. sim*, *D.mel*, and *Hmr* mutants from western blot signals in (B).

(D) Knockdown of *Hmr* or *Lhr* in *D.mel* cells results in a coreduction of HMR and LHR amounts.

(E) An additional autosomal copy of Hmr_{mel} leads to female hybrid lethality. #Crosses were performed with three times more virgins. *Male presumably exceptional, carrying a *D.sim* X chromosome.

mothers carrying an *Hmr*^{3} allele validates that the observed signal originates from HMR and is not due an antibody cross-reactivity to a *D.sim* protein (Figure S5B). It furthermore indicates that the HMR_{sim} level is dramatically reduced compared to that of HMR_{mel}, in line with the results in brain tissue and cell lines (Figures 6A and 6B). As the hypomorphic *Hmr*^{3} allele was generated by the insertion of a P element carrying UAS sites, it enables GAL4-mediated *Hmr* overexpression (Figures S5C–S5E). Salivary-gland-specific GAL4 expression triggering *Hmr* overexpression also results in HMR binding to numerous interband regions. Interestingly, these sites are often bordering and sometimes even overlapping with the male-specific lethal protein MSL2 (see Discussion) on the male X chromosome. Because HMR delocalizes after overexpression in *D.mel,* we would like to suggest that HMR mislocalization in hybrids is also the result of increased HMR levels.

DISCUSSION

Hmr_{mel} and Lhr_{sim} constitute members of a few identified examples of genes that form a classical Dobzhansky-Muller gene pair and mediate postzygotic isolation of the two closely related species *D.mel* and *D.sim* (Brideau et al., 2006; Davis et al., 1996). Here, we show that the gene products of *Hmr* and *Lhr* form a complex in *D.mel* with an important centromeric function. This function is exquisitely dose dependent as an increase as well as a decrease of complex levels result in an increased number of mitotic defects. At the same time, we also observe an increase in the number of transcripts derived from TEs upon alteration of the complex levels, suggesting that HMR/LHR has a function in setting up a repressive chromatin structure at these genomic regions. Although we cannot prove that the increased transcription from the transposable elements is the main cause for the mitotic defects, the centromeric binding pattern of the complex in mitotically cycling cells, its function in interphase, and the fact that a heterochromatic structure is beneficial for the generation of a functional centromere (Allshire et al., 1994; Olszak et al., 2011; Partridge et al., 2000) suggest that the HMR/LHR complex may contribute to a functional chromatin structure at the centromere. On first glance, the strong effects of an HMR depletion we see in cell culture as well as in fly strains expressing an *Hmr* RNAi construct would have predicted a stronger phenotype of *D.mel* flies carrying *Hmr* mutations than the one reported by Barbash and colleagues (Aruna et al., 2009). At least for the result in cell lines, we exclude off-target effects because we used two independently derived RNAi constructs with a similar outcome. In flies, it may well be that compensatory mechanisms can at least partially substitute HMRs function at centromeres, leading to a less pronounced effect. Compared to classical mutations, such compensatory effects are less frequent in knockdown experiments, which may also be the cause of the difference in viability.

Based on the fact that HMR and LHR show strong signatures of positive selection and an Hmr_{sim} transgene does not cause hybrid male lethality, Barbash and colleagues proposed that HMR_{mel} causes hybrid incompatibilities as a consequence of primary amino acid sequence divergence (Barbash et al., 2003; Maheshwari et al., 2008). Our evidence that the HMR/LHR complex is not crucial for proper centromere function in *D.sim* cells might partially lend support for such a functional divergence. On the other hand, the orthologs from both species behave virtually identical in all other tested assays. Considering that residues in HMR that are conserved between species are critical for hybrid lethality and that Hmr_{sim} can partially rescue the fertility defect of *D.mel Hmr* mutant females (Aruna et al., 2009), we would like to propose an alternative model. Our data strongly support a scenario, in which the asymmetric lethal effects of Hmr_{mel} and Lhr_{sim}, respectively, are due to the divergence in regulatory pathways that modulate their levels, which is the most apparent difference between the orthologs we could identify.

We can only speculate about the driving force that led to the increased expression of *Hmr* in *D.mel.* Considering our finding that HMR/LHR levels are critical for setting up a repressive chromatin structure at centromeric regions, it is striking that *D.sim* and *D.mel* strongly differ in the number of TEs, and these elements are highly enriched at centromeres (Bergman et al.,

2006; Sun et al., 1997, 2003). Interestingly, whereas most of the copies are degraded to small fragments in *D.sim*, *D.mel* contains substantially more intact copies (Lerat et al., 2011). This might be reflected in higher levels of HMR/LHR complex in *D.mel* and its crucial role in centromere functionality in tissues with mitotic cell cycles.

The species inverted higher expression of *Hmr* and *Lhr* results in increased complex amounts relative to its target sites, which are diluted in the hybrid genetic background. We propose that this misbalance results in the lethal gain of function in hybrids. This model also implicates that factors that influence the abundance of the complex are modifiers of hybrid lethality. In fact, early genetic experiments hinted toward such modifiers. For instance, hybrid males from *D.mel* mothers and *D.sim* fathers are not lethal if they carry two third chromosomes from *D.mel* (3_{mel}) (Pontecorvo, 1943). This implies that either a sensitizer locus on 3_{sim} or a haploinsufficient suppressor locus on 3_{mel} exists. We would favor the suppressor model, in which a negative regulator of complex abundance is diluted in hybrids. This hypothesis is based on the observation that LHR_{sim} does not require HMR_{sim} for its high levels in *D.sim*, but its abundance depends on the presence of HMR_{mel} in hybrids. This becomes apparent by the decreased level of LHR_{sim} in Hmr^3 mutant hybrids.

Complete lethality further requires the presence of the *D.mel* X chromosome as the sole presence of an autosomal copy of HMR_{mel} does not kill male hybrids carrying an X_{sim} (Barbash et al., 2000; Hutter et al., 1990; unpublished data). In this respect, it was already postulated that disturbed dosage compensation may cause hybrid male lethality due to species-specific divergence of the involved components (Rodriguez et al., 2007) (Pal-Bhadra et al., 2004). Rodriguez and colleagues demonstrated that the *D.mel* dosage compensation system shows particularly strong signatures of positive selection, which may render the *D.sim* DCC components incompetent to properly compensate the *D.mel* X chromosome. In contrast, Pal-Bhadra et al. postulated that a key component of dosage compensation is not expressed in the lethal hybrid males. Their conclusion was based on the failure to detect MSL2 on lethal hybrid male X chromosomes with an X_{mel}, but not with an X_{sim}. The latter findings are in contrast to our results (Figure 7E), as we detect X-chromosome-specific binding of MSL2 on X_{mel}/Y_{sim} hybrid male polytene chromosomes. This discrepancy might be due to a different fixation procedure or the use of a more sensitive antibody. It is important to note, however, that based on our data we cannot fully exclude the existence of subtle differences in DCC function in lethal male hybrids. Barbash genetically tested the possibility that impaired dosage compensation causes hybrid male inviability making use of different *D.mel* dosage compensation complex (DCC) mutants. He found that these mutations rather increase than decrease hybrid male viability (Barbash, 2010). Furthermore, considering that female hybrid lethality is higher at elevated temperatures in an *Hmr*-dependent manner, Barbash puts forward another plausible scenario in which hybrid lethality is caused by a disturbed chromatin state of X_{mel}. In fact, chromatin structure of the male X is known to be extremely sensitive toward the amount of heterochromatin proteins (Spierer et al., 2008; 2005). Strikingly, two of the factors that strongly affect X chromosome morphology (HP1a and Su(var)3-7) copurify with HMR and LHR. Alternatively, global HMR/LHR-induced changes in chromatin structure, increases in mitotic defects, or deregulation of TEs might trigger a cell-cycle checkpoint leading to the observed cell-cycle arrest (Bolkan et al., 2007).

In summary, our experiments underscore the importance of tight regulation of protein levels to sustain their functional capacity. We show that altered expression levels of the DM pair *Hmr* and *Lhr* in hybrids result in detrimental problems concerning centromere function and silencing of transposable elements. The combination of these defects finally results in the observed lethality of hybrids from *D.mel* und *D.sim*, whereby HMR and LHR contribute to the reproductive isolation of the two species.

EXPERIMENTAL PROCEDURES

An extended version of the experimental procedures can be found in the Supplemental Experimental Procedures.

Cloning

All plasmids are available on request. For full cloning details and oligonucleotide information, see the Supplemental Experimental Procedures.

GST-Fusion Protein Expression, Purification, and Assessment of Anti-HMR Antibody Specificity

Recombinant GST-HMR fusion proteins were expressed in *E. coli* BL21(DE3) and purified via GST-affinity purification according to the manufacturer's instructions (GE Healthcare). For assessing the specificity of the anti-HMR 2C10 antibody, GST-HMR fusion proteins were separated by SDS-PAGE and blotted onto a nitrocellulose membrane. The membrane was first probed with the anti-HMR 2C10 antibody, and signals were visualized using an HRP-coupled anti-rat secondary antibody and ECL detection (Bio-Rad). To normalize for unequal protein loading, the membrane was reprobed using a primary mouse anti-GST monoclonal antibody and a fluorescently labeled anti-mouse secondary antibody, which was detected using the Odyssey infrared fluorescent imaging system (LI-COR Biosciences).

Quantification of Western Blot Signal Intensities

Background corrected total signal intensity per band was quantified and normalized to the corresponding Tubulin signal intensities using the AIDA software package (Raytest).

Protein Purification and Mass Spectrometry

Ammonium sulfate nuclear extracts, FLAG purifications and protein identifications were done as described before (Abel et al., 2009). For quantitation, raw data were analyzed using the MaxQuant 1.2.2.5 software package. Identified proteins were considered as interation partners if their MaxQuant iBAQ values displayed an enrichment greater than 16-fold compared to control anti-FLAG purifications from Schneider cell nuclear extracts not expressing any FLAG-tagged protein.

Isolation of Larval Brains for Protein Extraction and Transposable Element Deregulation Analysis

Brains from third larvae were dissected in serum-free Schneider medium and collected in ice-cold Ephrussi and Beadle Ringer's (EBR) solution. For the preparation of extracts, brains were homogenized in RIPA buffer supplemented with MG-132 (Enzo Life Sciences) and 0.2 mM phenylmethanesulfonylfluoride, incubated on ice for 30 min, and frozen in liquid nitrogen. After thawing on ice, brain extracts were recovered by centrifugation, concentration was measured, and 10 μg per sample was analyzed by immunoblotting. For analysis of transposable element deregulation, brains collected in EBR, the collected brains were frozen in aliquots in liquid nitrogen and stored at −80°C until further processing. Care was taken that the collection of each individual aliquot of brains lasted no longer than 20 min. Approximately 50 brains (70 for hybrid males) were used for each replicate.

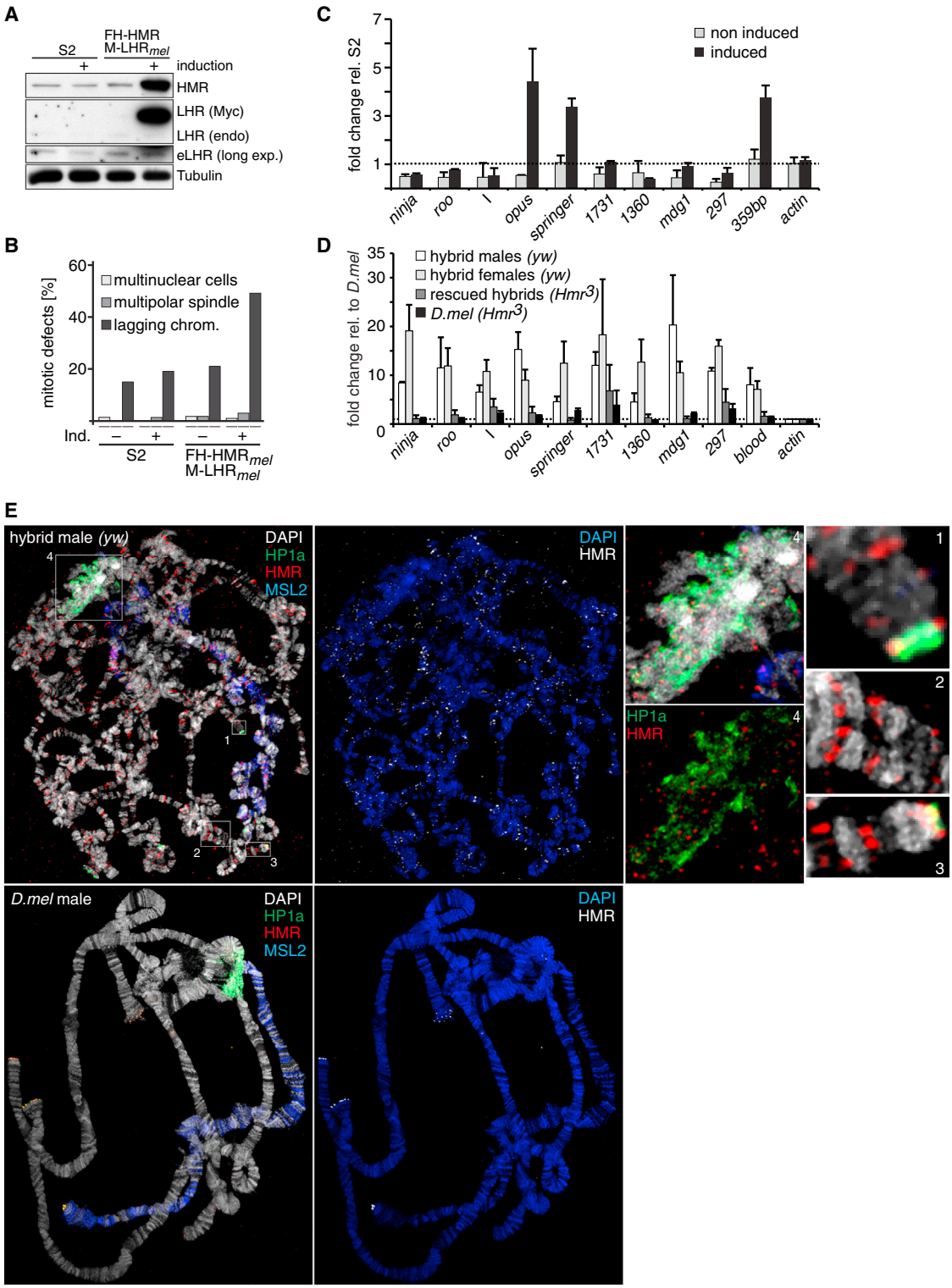

Figure 7. HMR/LHR Overexpression Provokes Mitotic Defects, Affects TE Regulation, and Leads to Global HMR Mislocalization in Hybrids

(A) Western blot demonstrating metallothionine promoter-driven FH-HMR$_{mel}$ and Myc-LHR$_{mel}$ overexpression upon copper sulfate treatment of stable *D.mel* cell lines.

(B) Quantification of the increase in mitotic defects upon FH-HMR$_{mel}$ and Myc-LHR$_{mel}$ overexpression. Given are the mean values from two independent experiments.

(C) Increase in TE transcript abundance upon HMR/LHR overexpression in *D.mel* cell lines.

(legend continued on next page)

Immunohistochemistry

For immunolocalization in tissue culture cells, cells were settled and fixed with PBS/3.7% paraformaldehyde at room temperature. Following permeabilization, cells were washed in PBS and blocked with image iT FX signal enhancer (Invitrogen). Antibodies were diluted and incubated with the coverslips overnight at 4°C. Following two washes with PBS/0.1% Triton X-100 (PBT), fluorophore-coupled-secondary antibodies were added. After PBT and PBS washes, stained cells were mounted in VECTASHIELD/DAPI (Vector Laboratories).

For immunostaining of wing imaginal discs third instar larvae were dissected in *Drosophila* Schneider medium, leaving discs attached to the carcass, rinsed in PBS, and fixed in PBS/4% paraformaldehyde. Following two washes in PBT, the tissue was permeabilized and blocked in PBT/5% normal goat serum (PBTN). Antibodies were diluted in PBTN, and tissues were stained for 3–4 days rotating at 4°C. After extensive PBTN washes, secondary antibodies diluted in PBTN were added. After extensive washes in PBT and PBS, discs were dissected away from carcass and mounted in VECTASHIELD/DAPI (Vector Labs).

For immunostaining of polytene chromosomes, salivary glands from third instar larvae were prepared in PBS, prefixed in PBT/3.7% formaldehyde for 3 min, incubated in 50% acetic acid/0.1% Triton X-100/3.7% formaldehyde for 165 s, and spread onto poly-L-lysine coated microscope slides. Suitable spreads were frozen in liquid nitrogen and stored overnight at −20°C in methanol. After 15 min rehydration in PBS, slides were blocked with image iT FX signal enhancer (Invitrogen). Primary antibodies were diluted in PBTN and incubated overnight at 4°C. Following two washes with PBT and another 30 min blocking step in PBT/1% BSA, fluorophore-coupled-secondary antibodies diluted in PBTN were added. After PBT washes, preparations were stained with DAPI, washed in PBS, and mounted in VECTASHIELD (Vector Labs). The polytene chromosome images in Figures 7E, S5A, and S5B were recorded and processed with identical settings to ensure their comparability.

Images were acquired using a Leica TCS SP5 confocal microscope with a 63× glycerol immersion objective NA = 1.3. Z stacks were deconvolved using the Huygens Essential Software (SVI). All other digital image processing and slight linear adjustment of brightness and contrast were done using ImageJ. If not stated otherwise in the figure legends, images are maximum intensity projections.

Analysis of Incorporation of Newly Synthesized SNAP-Cid

The assay was done as described in Chen et al. (2012).

Antibodies

HMR-specific antibodies were raised in Lou/c rats against a fragment spanning amino acids 2–416 fused to an N-terminal GST tag. For LHR-specific antibodies, MBP-LHR full length served as antigen. The DHMR 2C10 (rat IgG2b) rat-monoclonal antibody was used for all experiments except those displayed in Figures 1E and 1F. For the HMR/LHR costaining in Figure 1E, an HMR-specific mouse polyclonal serum was used. For staining of imaginal discs (Figure 1F), a mixture of the DHMR-specific monoclonal antibodies 3D8 (rat IgG2a) and 2C10 was used to increase sensitivity. Anti-LHR immunoblots in Figures 6B and S4C were performed with the DLHR 20G3 (rat IgG2b) rat monoclonal antibody that recognizes LHR-*mel* and LHR-*sim* with similar efficiency. All other experiments were performed with the DLHR antibody 12F4 (rat IgG2a) specific for LHR-*mel*. The following antibodies were kindly provided by other investigators: rabbit anti-MSL2 (Peter Becker), guinea-pig anti-HOAP (Jamy Peng), rabbit anti-Cenp-C (Christian Lehner), rabbit anti-HP1a Serum (Sarah Elgin), chicken anti-Ndc80 (Tom Mareska), and mouse anti-Polo (Claudio Sunkel). The rat anti-incenp antibody was produced in house, using an amino-terminal fragment cloned by Mar Carmena. The mouse anti-GST monoclonal 2C8 and the rat anti-CID 7A2 (rat IgG2a) antibodies were obtained from the monoclonal antibody facility of the Helmholtz Center Munich. The mouse anti-HP1a C1A9 was obtained from the Developmental Studies Hybridoma Bank (DHSB). The following antibodies are commercially available: rabbit anti-histone H3 phospho S10 (Abcam), mouse anti-FLAG M2 (Roche), rat anti-HA 3F10 (Roche), mouse anti-Myc 9E10 (Roche), monoclonal mouse anti-alpha-Tubulin (Sigma), and rabbit anti-Cid (Active Motif).

Cell Culture and RNAi

Growth of cells: the *Drosophila* Schneider Line 2 derivative L2–4 was used for all experiments with *D.mel* cells. *D.sim* embryonic cells (Yoshioka et al., 1992) were obtained from the DGRC. The GFP-Cid cell line is described in Olszak et al. (2011); the SNAP-Cid cell line was provided by Gary Karpen. All cells were grown at 26°C in Schneider medium (Invitrogen) supplemented with 10% fetal calf serum and penicillin/streptomycin.

Generation of Stable Cell Lines

For the generation of stable cell lines, cells were transfected using Effectene (QIAGEN) or XtremeGENE HP (Roche) according to the manufacturer's instructions and selected for 4 weeks with 250 μg/ml Hygromycin B (Invitrogen). Expression of the transgenes was verified by western blotting and immunofluorescence analysis. Expression of proteins was induced by adding copper sulfate to a final concentration of 250 μM 24–48 hr before harvest of cells. RNAi experiments and the scoring of mitotic defects were essentially done as described (Heun et al., 2006; Padeken et al., 2013).

Fly Culture and Crosses

Flies were raised on standard cornmeal/yeast extract medium at 25°C except hybrid crosses, which were performed at 21°C. *yw*, Hmr^{3}, Hmr^{1}, C167.4 (*D.sim*), and GAL4 driver lines were obtained from the Bloomington Stock Center. Inducible RNAi lines were received from the VDRC (Vienna). The transgenic line carrying an autosomal wild-type Hmr_{mel} allele ($Hmr^{+t9.5}$) was generated by BestGene using *PhiC31*-integrase-mediated integration of a 9.5 kbp genomic fragment containing construct, spanning the entire Hmr_{mel} gene as well as parts of the flanking CG2124 and Rab9D genes. The genotype of the parental line was $y^{1}\ w^{67c23}$; *P{CaryP}attP40*.

Analysis of Transposable Element Derepression

The analysis of transposable element derepression was done as described in Padeken et al. (2013).

ACCESSION NUMBERS

The mass spectrometry data for the HMR, LHR, and tandem purifications have been deposited to the ProteomeXchange Consortium (http://proteomecentral.proteomexchange.org) via the PRIDE partner repository and accession codes with the data set identifier PXD000489.

SUPPLEMENTAL INFORMATION

Supplemental Information includes Supplemental Experimental Procedures, five figures, one table, and one movie and can be found with this article online at http://dx.doi.org/10.1016/j.devcel.2013.10.001.

ACKNOWLEDGMENTS

This work was funded by grants from the European Union (EpiGeneSys, 257082) and the Deutsche Forschungsgemeinschaft (DFG; Projekt IM 23/9-1) to A.I. and an ERC grant to P.H. (ERC-BioSynCen). J.P. and P.H. were supported by the Max Planck Society and GOMS by the Deutsche Forschungsgemeinschaft (DFG; Projekt HE 3434/2-1). We thank Matthias Prestel for initial help regarding fly crossings and all members of the Imhof group for

(D) Hmr_{mel}-dependent increase in transposable element transcription in hybrid larval brains. In (C) and (D), mean values and range bars from two biological replicates are given.

(E) Mislocalization of HMR on hybrid male (upper panel) versus *D.mel yw* male (lower panel) polytene chromosomes. The genotype of the *D.mel* mother is given in brackets. Enlarged images of boxed regions (numbered from 1 to 4) are shown next to the overview images.

See also Figure S5.

critical reading of the manuscript and comments and the PRIDE Team for help with data deposition on the proteome exchange server.

Received: May 23, 2013
Revised: August 26, 2013
Accepted: October 1, 2013
Published: November 14, 2013

REFERENCES

Abel, J., Eskeland, R., Raffa, G.D., Kremmer, E., and Imhof, A. (2009). Drosophila HP1c is regulated by an auto-regulatory feedback loop through its binding partner Woc. PLoS ONE *4*, e5089.

Allshire, R.C., Javerzat, J.P., Redhead, N.J., and Cranston, G. (1994). Position effect variegation at fission yeast centromeres. Cell *76*, 157–169.

Aruna, S., Flores, H.A., and Barbash, D.A. (2009). Reduced fertility of Drosophila melanogaster hybrid male rescue (Hmr) mutant females is partially complemented by Hmr orthologs from sibling species. Genetics *181*, 1437–1450.

Baker, B. (1989). Genes controlling essential cell-cycle functions in Drosophila melanogaster. Genes Dev. *3*, 438–453.

Barbash, D.A. (2010). Genetic testing of the hypothesis that hybrid male lethality results from a failure in dosage compensation. Genetics *184*, 313–316.

Barbash, D.A., Roote, J., and Ashburner, M. (2000). The Drosophila melanogaster hybrid male rescue gene causes inviability in male and female species hybrids. Genetics *154*, 1747–1771.

Barbash, D.A., Siino, D.F., Tarone, A.M., and Roote, J. (2003). A rapidly evolving MYB-related protein causes species isolation in Drosophila. Proc. Natl. Acad. Sci. USA *100*, 5302–5307.

Bayes, J.J., and Malik, H.S. (2009). Altered heterochromatin binding by a hybrid sterility protein in Drosophila sibling species. Science *326*, 1538–1541.

Bergman, C.M., Quesneville, H., Anxolabéhère, D., and Ashburner, M. (2006). Recurrent insertion and duplication generate networks of transposable element sequences in the Drosophila melanogaster genome. Genome Biol. *7*, R112.

Bolkan, B.J., Booker, R., Goldberg, M.L., and Barbash, D.A. (2007). Developmental and cell cycle progression defects in Drosophila hybrid males. Genetics *177*, 2233–2241.

Brideau, N.J., and Barbash, D.A. (2011). Functional conservation of the Drosophila hybrid incompatibility gene Lhr. BMC Evol. Biol. *11*, 57.

Brideau, N.J., Flores, H.A., Wang, J., Maheshwari, S., Wang, X., and Barbash, D.A. (2006). Two Dobzhansky-Muller genes interact to cause hybrid lethality in Drosophila. Science *314*, 1292–1295.

Brown, J.D., and O'Neill, R.J. (2010). Chromosomes, conflict, and epigenetics: chromosomal speciation revisited. Annu. Rev. Genomics Hum. Genet. *11*, 291–316.

Chen, E.S., Zhang, K., Nicolas, E., Cam, H.P., Zofall, M., and Grewal, S.I.S. (2008). Cell cycle control of centromeric repeat transcription and heterochromatin assembly. Nature *451*, 734–737.

Chen, C.-C., Greene, E., Bowers, S.R., and Mellone, B.G. (2012). A role for the CAL1-partner Modulo in centromere integrity and accurate chromosome segregation in Drosophila. PLoS ONE *7*, e45094.

Crespi, B., and Nosil, P. (2013). Conflictual speciation: species formation via genomic conflict. Trends Ecol. Evol. *28*, 48–57.

Czech, B., Malone, C.D., Zhou, R., Stark, A., Schlingeheyde, C., Dus, M., Perrimon, N., Kellis, M., Wohlschlegel, J.A., Sachidanandam, R., et al. (2008). An endogenous small interfering RNA pathway in Drosophila. Nature *453*, 798–802.

Dalal, Y., Furuyama, T., Vermaak, D., and Henikoff, S. (2007). Structure, dynamics, and evolution of centromeric nucleosomes. Proc. Natl. Acad. Sci. USA *104*, 15974–15981.

Davis, A.W., Roote, J., Morley, T., Sawamura, K., Herrmann, S., and Ashburner, M. (1996). Rescue of hybrid sterility in crosses between D. melanogaster and D. simulans. Nature *380*, 157–159.

Dobzhansky, T. (1951). Genetics and the Origin of Species. (New York: Columbia University Press).

Fishman, L., and Saunders, A. (2008). Centromere-associated female meiotic drive entails male fitness costs in monkeyflowers. Science *322*, 1559–1562.

Greil, F., de Wit, E., Bussemaker, H.J., and van Steensel, B. (2007). HP1 controls genomic targeting of four novel heterochromatin proteins in Drosophila. EMBO J. *26*, 741–751.

Hedges, D.J., and Belancio, V.P. (2011). Restless genomes humans as a model organism for understanding host-retrotransposable element dynamics. Adv. Genet. *73*, 219–262.

Heun, P., Erhardt, S., Blower, M.D., Weiss, S., Skora, A.D., and Karpen, G.H. (2006). Mislocalization of the Drosophila centromere-specific histone CID promotes formation of functional ectopic kinetochores. Dev. Cell *10*, 303–315.

Hutter, P., and Ashburner, M. (1987). Genetic rescue of inviable hybrids between Drosophila melanogaster and its sibling species. Nature *327*, 331–333.

Hutter, P., Roote, J., and Ashburner, M. (1990). A genetic basis for the inviability of hybrids between sibling species of Drosophila. Genetics *124*, 909–920.

Kharchenko, P.V., Alekseyenko, A.A., Schwartz, Y.B., Minoda, A., Riddle, N.C., Ernst, J., Sabo, P.J., Larschan, E., Gorchakov, A.A., Gu, T., et al. (2011). Comprehensive analysis of the chromatin landscape in Drosophila melanogaster. Nature *471*, 480–485.

Khurana, J.S., Wang, J., Xu, J., Koppetsch, B.S., Thomson, T.C., Nowosielska, A., Li, C., Zamore, P.D., Weng, Z., and Theurkauf, W.E. (2011). Adaptation to P element transposon invasion in Drosophila melanogaster. Cell *147*, 1551–1563.

Kidwell, M.G., Kidwell, J.F., and Sved, J.A. (1977). Hybrid dysgenesis in Drosophila melanogaster: a syndrome of aberrant traits including mutation, sterility and male recombination. Genetics *86*, 813–833.

Lerat, E., Burlet, N., Biémont, C., and Vieira, C. (2011). Comparative analysis of transposable elements in the melanogaster subgroup sequenced genomes. Gene *473*, 100–109.

Long, Y., Zhao, L., Niu, B., Su, J., Wu, H., Chen, Y., Zhang, Q., Guo, J., Zhuang, C., Mei, M., et al. (2008). Hybrid male sterility in rice controlled by interaction between divergent alleles of two adjacent genes. Proc. Natl. Acad. Sci. USA *105*, 18871–18876.

Maheshwari, S., and Barbash, D.A. (2012). Cis-by-Trans regulatory divergence causes the asymmetric lethal effects of an ancestral hybrid incompatibility gene. PLoS Genet. *8*, e1002597.

Maheshwari, S., Wang, J., and Barbash, D.A. (2008). Recurrent positive selection of the Drosophila hybrid incompatibility gene Hmr. Mol. Biol. Evol. *25*, 2421–2430.

Malik, H.S., and Henikoff, S. (2001). Adaptive evolution of Cid, a centromere-specific histone in Drosophila. Genetics *157*, 1293–1298.

Malik, H.S., and Henikoff, S. (2009). Major evolutionary transitions in centromere complexity. Cell *138*, 1067–1082.

Mellone, B.G., Grive, K.J., Shteyn, V., Bowers, S.R., Oderberg, I., and Karpen, G.H. (2011). Assembly of Drosophila centromeric chromatin proteins during mitosis. PLoS Genet. *7*, e1002068.

Mihola, O., Trachtulec, Z., Vlcek, C., Schimenti, J.C., and Forejt, J. (2009). A mouse speciation gene encodes a meiotic histone H3 methyltransferase. Science *323*, 373–375.

Olszak, A.M., van Essen, D., Pereira, A.J., Diehl, S., Manke, T., Maiato, H., Saccani, S., and Heun, P. (2011). Heterochromatin boundaries are hotspots for de novo kinetochore formation. Nat. Cell Biol. *13*, 799–808.

Padeken, J., Mendiburo, M.J., Chlamydas, S., Schwarz, H.-J., Kremmer, E., and Heun, P. (2013). The nucleoplasmin homolog NLP mediates centromere clustering and anchoring to the nucleolus. Mol. Cell *50*, 236–249.

Pal-Bhadra, M., Leibovitch, B.A., Gandhi, S.G., Chikka, M.R., Bhadra, U., Birchler, J.A., and Elgin, S.C.R. (2004). Heterochromatic silencing and HP1 localization in Drosophila are dependent on the RNAi machinery. Science *303*, 669–672.

Pardo-Manuel de Villena, F., and Sapienza, C. (2001). Female meiosis drives karyotypic evolution in mammals. Genetics *159*, 1179–1189.

Partridge, J.F., Borgstrøm, B., and Allshire, R.C. (2000). Distinct protein interaction domains and protein spreading in a complex centromere. Genes Dev. *14*, 783–791.

Phadnis, N., and Orr, H.A. (2009). A single gene causes both male sterility and segregation distortion in Drosophila hybrids. Science *323*, 376–379.

Pontecorvo, G. (1943). Viability interactions between chromosomes ofDrosophila melanogaster andDrosophila simulans. J. Genet. *45*, 51–66.

Rodriguez, M.A., Vermaak, D., Bayes, J.J., and Malik, H.S. (2007). Species-specific positive selection of the male-specific lethal complex that participates in dosage compensation in Drosophila. Proc. Natl. Acad. Sci. USA *104*, 15412–15417.

Ross, B.D., Rosin, L., Thomae, A.W., Hiatt, M.A., Vermaak, D., de la Cruz, A.F., Imhof, A., Mellone, B.G., and Malik, H.S. (2013). Stepwise evolution of essential centromere function in a Drosophila neogene. Science *340*, 1211–1214.

Schartl, M. (2008). Evolution of Xmrk: an oncogene, but also a speciation gene? Bioessays *30*, 822–832.

Scott, K.C., Merrett, S.L., and Willard, H.F. (2006). A heterochromatin barrier partitions the fission yeast centromere into discrete chromatin domains. Curr. Biol. *16*, 119–129.

Scott, K.C., White, C.V., and Willard, H.F. (2007). An RNA polymerase III-dependent heterochromatin barrier at fission yeast centromere 1. PLoS ONE *2*, e1099.

Spierer, A., Seum, C., Delattre, M., and Spierer, P. (2005). Loss of the modifiers of variegation Su(var)3-7 or HP1 impacts male X polytene chromosome morphology and dosage compensation. J. Cell Sci. *118*, 5047–5057.

Spierer, A., Begeot, F., Spierer, P., and Delattre, M. (2008). SU(VAR)3-7 links heterochromatin and dosage compensation in Drosophila. PLoS Genet. *4*, e1000066.

Sturtevant, A.H. (1920). Genetic studies on Drosophila simulans. I. Introduction. Hybrids with Drosophila melanogaster. Genetics *5*, 488–500.

Sun, X., Wahlstrom, J., and Karpen, G. (1997). Molecular structure of a functional Drosophila centromere. Cell *91*, 1007–1019.

Sun, X., Le, H.D., Wahlstrom, J.M., and Karpen, G.H. (2003). Sequence analysis of a functional Drosophila centromere. Genome Res. *13*, 182–194.

Tang, S., and Presgraves, D.C. (2009). Evolution of the Drosophila nuclear pore complex results in multiple hybrid incompatibilities. Science *323*, 779–782.

Vermaak, D., and Malik, H.S. (2009). Multiple roles for heterochromatin protein 1 genes in Drosophila. Annu. Rev. Genet. *43*, 467–492.

Watanabe, T.K. (1979). A gene that rescues the lethal hybrids between *Drosophila melanogaster* and *D. simulans*. Jpn. J. Genet. *54*, 325–331.

Yoshioka, K., Kanda, H., Takamatsu, N., Togashi, S., Kondo, S., Miyake, T., Sakaki, Y., and Shiba, T. (1992). Efficient amplification of Drosophila simulans copia directed by high-level reverse transcriptase activity associated with copia virus-like particles. Gene *120*, 191–196.